AD666053

AFCRL-68-0018

ON THE INCLUSION OF LONG-WAVE RADIATION IN A TROPOSPHERIC NUMERICAL PREDICTION MODEL

Maurice B. Danard
Dept. of Meteorology and Oceanography
Naval Postgraduate School
Monterey, California

Research Project MIPR ES-7-967
Project No. 6698
Task No. 669802
Work Unit No. 66980201

Scientific Report No. 1
January 1968

Contract Monitor: Thomas Keegan, Meteorology Laboratory

Distribution of this document is unlimited. It may be released to the Clearing House, Department of Commerce, for sale to the general public.

DDC
MAR 13 1968
UNCLASSIFIED

Prepared for

AIR FORCE CAMBRIDGE RESEARCH LABORATORIES
OFFICE OF AEROSPACE RESEARCH
UNITED STATES AIR FORCE
BEDFORD, MASSACHUSETTS 01730

MAR 1968
RECEIVED
NASA STI FACILITY
INPUT BRANCH

Reproduced by the
CLEARINGHOUSE
for Federal Scientific & Technical
Information Springfield Va. 22151

AFCRL-68-0018

ON THE INCLUSION OF LONG-WAVE RADIATION IN A TROPOSPHERIC NUMERICAL PREDICTION MODEL

Maurice B. Danard
Dept. of Meteorology and Oceanography
Naval Postgraduate School
Monterey, California

Research Project MIPR ES-7-967
Project No. 6698
Task No. 669802
Work Unit No. 66980201

Scientific Report No. 1
January 1968

Contract Monitor: Thomas Keegan, Meteorology Laboratory

Distribution of this document is unlimited. It may be released to the Clearing House, Department of Commerce, for sale to the general public.

Prepared for

AIR FORCE CAMBRIDGE RESEARCH LABORATORIES
OFFICE OF AEROSPACE RESEARCH
UNITED STATES AIR FORCE
BEDFORD, MASSACHUSETTS 01730

NAVAL POSTGRADUATE SCHOOL
Monterey, California

Rear Admiral R. W. McNitt, USN
Superintendent

R. F. Rinehart
Academic Dean

This task was supported by: U. S. Air Force Cambridge Research Laboratories
Research Project MIPR ES-7-967

Maurice B. Danard
Maurice B. Danard
Associate Professor of Meteorology

Approved by:

G. J. Haltiner
G. J. Haltiner
Chairman
Department of Meteorology
and Oceanography

Released by:

C. E. Menneken
C. E. Menneken
Dean of Research Administration

NPS-51DD8011A
January 1968

Abstract

A simple method of computing long-wave radiative cooling in the troposphere associated with water vapor is described. Radiation from ozone and carbon dioxide is not considered. However, influences of arbitrary vertical distributions of cloud and moisture are included.

Average annual cooling rates along a meridional cross-section are calculated for a cloudless atmosphere. The results agree fairly well with the total radiative cooling (long- and short-wave) as given by Manabe and Moller (1961) except in the lower troposphere at low latitudes. Here short-wave absorption by water vapor is appreciable.

Long-wave radiative cooling is also computed in a case of a developing cyclone for comparison with release of latent heat. The largest cooling occurs at cloud top and can be a significant fraction of the amount of energy released as latent heat in the upper troposphere. Destabilization of the cloud mass and subsequent increase in precipitation may be important in cyclone development.

1. Introduction

The heat budget of the atmosphere may be partitioned as follows: (1) absorption of short-wave radiation, (2) sensible heat transfer from the earth's surface by conduction and convection, (3) release of latent heat, and (4) absorption and emission of long-wave radiation. Of these, long-wave radiation is the most important term in the mean tropospheric heat budget (see, e.g., Davis 1960 or London 1957). Release of latent heat is, on the average, the second most important term. However, it is often locally predominant in areas of precipitation and its inclusion in a prediction model appears desirable in forecasting cyclogenesis (Danard 1964, 1966a, 1966b).

This paper describes a simple method of including long-wave radiation from water vapor in a tropospheric numerical model which predicts the field of moisture. Radiation from ozone and carbon dioxide is not considered. However, effects of arbitrary vertical distributions of cloud and moisture are included.

Using a numerical model incorporating release of latent heat but not long-wave radiation, the author (Danard 1966a, 1966b) noted a tendency for predicted heights to be too high in the upper troposphere. This may have been due to neglect of long-wave cooling from cloud tops. Inclusion of long-wave radiation should extend the viability of such models.

2. Theory and basic procedure

Since flux divergence associated with carbon dioxide is usually small in the troposphere (see, e.g., Manabe and Moller (1961), or Manabe and Strickler (1964)), only water vapor will be considered. Computations will be performed for the atmosphere below some level p_u (near the tropopause). This is the highest level for which meteorological variables are assumed known.

Results of Kuhn (1963c) suggest the following expression for the corrected precipitable water or path length between p=0 and p=p:

$$w = \frac{1}{g} \int_o^p q \left\{ \frac{p}{p_o} \right\}^{0.85} \left\{ \frac{T_o}{T} \right\}^{0.5} dp \qquad (1)$$

Here p_o and T_o denote standard pressure and temperature, and q is the specific humidity. w may be regarded as a vertical coordinate increasing downward.

In computing w_u, the value of w at $p=p_u$, use is made of Manabe and Moller's (1961) observation that the frost point in the lower stratosphere is about 190 K irrespective of season and latitude. This value is attained at a height of about 15 km or 120 mb. Assume that the layer above p_u is isothermal with temperature T_u. Setting T_u=220 K, (1) then gives a value for w from p=0 to p=120 mb of 4.6×10^{-7} gm cm^{-2}. Assume that q varies linearly with pressure from p=120 mb to $p=p_u$. With the aid of (1), this permits us to compute the contribution to w from the layer between these levels. Adding this to the contribution from the layer above yields (in cgs units)

$$w_u = 4.7 \times 10^{-5} + 9.9\, q_u \qquad (2)$$

where q_u is the value of q at $p=p_u$. Note that w_u normally decreases from equator to pole.

The net flux (positive downward) at a level p* between cloud layers (see Fig. 1) is

$$F^* = F_{ba} - F_{bc} + \int_{w_a}^{w^*} \{F_{bw} - F_{ba}\}\epsilon'(w^*-w)dw + \int_{w^*}^{w_c} \{F_{bc} - F_{bw}\}\epsilon'(w-w^*)dw \tag{3}$$

where F_{bw}, F_{ba} and F_{bc} are the black body fluxes corresponding to the temperature at w, w_a and w_c, and $\epsilon'(w^*-w)$ is the rate of change of emissivity ϵ with path length evaluated at a path length (w^*-w) (corresponding to the slab between w and w*). Throughout this paper, arguments of functions are enclosed in parentheses ( ). A similar equation is given by Kuhn (1963a). If the level p* is in cloud, F* is assumed zero. If no cloud exists above p*, $w_a=0$ and $F_{ba}=0$. Eq. (3) is derived in a manner similar to that described by, e.g., Haltiner and Martin (1957, pp. 85-86). An outline of the derivation is given in the remainder of this paragraph. The flux in the spectral interval λ to $\lambda + d\lambda$ at w* from the black body surface at w_a is

$$dF^*\downarrow_{a\lambda} = 2F_{ba\lambda} H_3(k_\lambda \{w^* - w_a\}) \tag{4}$$

where $H_n(x) = \int_0^\infty e^{-xy} y^{-n} dy$, $F_{ba\lambda}$ is the black body flux at w_a in the spectral interval λ to $\lambda + d\lambda$, k_λ is the absorption coefficient and λ is the wave-length. The flux at w* from the stratum between

w_a and w^* is

$$dF^{*\downarrow}_{w\lambda} = 2k_\lambda \int_{w_a}^{w^*} F_{bw\lambda} H_2(k_\lambda\{w^*-w\})dw \tag{5}$$

where $F_{bw\lambda}$ is the black body flux at w in the spectral interval λ to $\lambda + d\lambda$. Now

$$H_3(k_\lambda\{w^*-w_a\}) = \tfrac{1}{2} - k_\lambda \int_{w_a}^{w^*} H_2(k_\lambda\{w^*-w\})dw \tag{6}$$

Adding (4) and (5), making use of (6), and integrating over all wavelengths yields

$$F^{*\downarrow} = F_{ba} - 2\int_{w_a}^{w^*}\int_0^\infty k_\lambda F_{ba\lambda} H_2(k_\lambda\{w^*-w\})d\lambda\, dw$$

$$+ 2\int_{w_a}^{w^*}\int_0^\infty k_\lambda F_{bw\lambda} H_2(k_\lambda\{w^*-w\})d\lambda\, dw \tag{7}$$

Now for an isothermal slab,

$$\epsilon'(w^*-w) = \frac{2}{F_{bw}} \int_0^\infty k_\lambda F_{bw\lambda} H_2(k_\lambda\{w^*-w\})d\lambda \tag{8}$$

Eq. (8) is derived by, e.g., Brooks (1950). It may also be obtained

from (5). For a fixed value of (w*-w), ϵ and therefore ϵ' as well will be assumed independent of temperature. This is because the temperature dependence has already been included in (1), which is used to compute w and w*. Hence (8) will be assumed to apply also when the temperature varies between w and w*. Thus the last term on the right side of (7) is $\int_{w_a}^{w^*} F_{bw}\epsilon'(w^*-w)dw$. Making the approximation

$F_{ba\lambda}/F_{ba} = F_{bw\lambda}/F_{bw}$ (i.e., for a fixed wavelength, $F_{b\lambda}/F_b$ is assumed to vary little over the range of tropospheric temperatures), the second term on the right side of (7) becomes $-F_{ba}\int_{w_a}^{w^*}\epsilon'(w^*-w)dw$.

Hence (7) gives the first and third terms on the right side of (3). Similar calculations show that the contributions from the black body surface at w_c and the layer between w* and w_c are represented by the second and final terms on the right of (3).

The assumption that a cloud surface behaves as a black body is probably justified for water droplet clouds at low elevations. For example, Kuhn (1963a) measured the emissivity of an overcast stratocumulus cloud deck with base at 900 mb and top at 855 mb. He obtained the value of 0.98. As Kuhn's results indicate, however, the attumption is less realistic for clouds at higher elevations. For a 9/10 sky cover of cirrostratus with base at 235 mb and top at 160 mb, the computed emissivity was 0.59.

The heating rate associated with radiation is given by

$$\left(\frac{\partial T}{\partial t}\right)_r = -\frac{g}{c_p}\frac{\partial F^*}{\partial p} \qquad (9)$$

3. Adaptation to a numerical model

For purposes of illustration, the model described in Section 2 will be adapted to a primitive equations numerical model developed by Krishnamurti. However, it could be modified to any model in which a moisture parameter is predicted.

The level p_u is taken as 200 mb and Eq. (2) is used to compute w_u. Eq. (3) is evaluated at 200, 400, 600, 800 and 1000 mb (Fig. 2). The integrals are computed by summation over 200 mb thick layers. For example,

$$\int_{w_a}^{w^*} \{F_{bw}-F_{ba}\}\epsilon'(w^*-w)dw = \Sigma \{\bar{F}_{bw}-F_{ba}\}\{\epsilon(w^*-w_t)-\epsilon(w^*-w_b)\} \qquad (10)$$

Here w_t and w_b are the values of w at the top and bottom of the 200 mb thick contributing layer, and $\bar{F}_{bw}$ is the black body flux at the mid-point. The summation extends over all layers between w_a and w*. Similarly,

$$\int_{w^*}^{w_c} \{F_{bc}-F_{bw}\}\epsilon'(w-w^*)dw = \Sigma \{F_{bc}-\bar{F}_{bw}\}\{\epsilon(w_b-w^*)-\epsilon(w_t-w^*)\} \qquad (11)$$

In (11), the summation extends over layers between w* and w_c. Kuhn (1963b) employed a similar method of computation.

Cloud is assumed to exist at a given level if

$$q/q_s > r(p) \qquad (12)$$

where q_s is the saturation specific humidity and r(p) is a critical value for existence of cloud. Table 1 gives values of r(p) adapted from Smagorinsky's (1960) relations between relative humidity and cloud

Table 1. Values of r(p) (see Eq. (12)) for existence of cloud (adapted from Smagorinsky 1960).

p(mb)	900	700	500	300
r(p)	0.84	0.75	0.70	0.69

amount. The values in the table correspond to 8/10 cloud at the given level. Relation (12) is tested at 300, 500, 700 and 900 mb, with the cloud (if it exists) corresponding to each level assumed to be 200 mb thick. The model atmosphere can thus have sixteen configurations of cloud ranging from completely cloud-free to cloudy at all four levels (Fig. 3)

Kuhn's (1963c) values of ϵ are used.

In the computer programming of Eq. (3), F* is first set equal to zero at the five levels indicated in Fig. 2. Then it is evaluated from 200 mb down to the top of the highest cloud (or the earth's surface). This means that at this stage flux computations are complete for configurations 1-5 of Fig. 3. Next, F* is computed from the base of the highest cloud down to the top of the next highest cloud (or the earth's surface). This completes calculations for configurations 6-15. Finally, F* is computed at the 800 and 1000 mb levels of configuration 16 to finish the flux computations.

Eq. (9) is evaluated at 300, 500, 700 and 900 mb by expressing $\partial F^*/\partial p$ as a finite difference over layers 200 mb thick (see Fig. 2).

4. Application to a mean meridional cross-section

Manabe and Moller (1961) compute the annual average cooling rates associated with radiation as a function of height and latitude for the northern hemisphere. They include long and short-wave absorption by ozone, carbon dioxide and water vapor and neglect the effects of clouds.

Since only long-wave absorption by water vapor is included in the method presented in this paper, it is of interest to compare the tropospheric cooling rates thus computed with those of Manabe and Moller.

Using the mean values of temperature and pressure compiled by London (1957), Eq. (3) was evaluated at 1 km intervals from the surface to 12 km. London's humidity values were accepted for $T > -30$ C. However, at lower temperatures, a constant frost-point lapse rate of 6.25 C km^{-1} was assumed. This was also done by Manabe and Moller. Eq. (2) was used to compute w_u and p_u was taken as 200 mb. For comparison with Manabe and Moller's results, the atmosphere was assumed cloud-free. Cooling rates were computed at 0.5, 1.5,...., 11.5 km. Average annual values, which have been smoothed slightly, are presented in Fig. 4. Fig. 4 may be compared with Fig. 21 of Manabe and Moller (1961). The two figures are fairly similar. The average cooling rate in Fig. 4 is 1.1 C day^{-1} compared to 0.9 C day^{-1} for Manabe and Moller's results for the same region. Differences between the results of this paper and those of Manabe and Moller may be seen in Fig. 5. It will be seen that considering just long-wave radiation from water vapor tends to overestimate the total radiative cooling (long- and short-wave) at low latitudes and low levels. The discrepancy is probably due to short-wave absorption by water vapor.

Results of Davis (1963) indicate that in such regions this absorption can be half as large as the long-wave cooling.

Goody (1964, p. 272) states that cooling rates computed from different techniques may vary by as much as 50 per cent. In view of this remark and the assumptions made in the present paper, the agreement with Manabe and Moller's results must be considered as reasonably good. Note that the above comparison is not simply a test of the method used to compute long-wave radiation from water vapor. It is primarily an assessment of the validity of omitting short-wave radiation as well as long-wave radiation from carbon dioxide and ozone in the troposphere.

Fig. 4 may also be compared with the infrared cooling rates of London (1957). However, London accounted for average cloudiness whereas in the present study the atmosphere was assumed cloud-free.

5. Comparison with release of latent heat

The author has previously calculated the spatial distribution of release of latent heat at 400, 600 and 800 mb in a developing cyclone over the United States (Danard 1964). To permit a comparison between these results and long-wave radiative effects, the method described in Section 3 was modified somewhat. The level p_u was taken as 300 mb and T_u was assigned the value 230 K. An equation similar to (2) but applicable here is

$$w_u = 5.0 \times 10^{-5} + 28\, q_u \qquad (13)$$

The 900 mb surface was assumed to be a black body. Eq. (3) was then evaluated at 300, 500, 700 and 900 mb, and cooling rates were computed at 400, 600 and 800 mb. Existence of cloud at these levels was deduced using values of r(p) (see (12)) obtained in the same manner as those in Table 1. Surface observations of clouds were also utilized. In other respects, the procedures of Section 3 were followed.

Results are presented in Figs. 6-9. The reader is referred to the paper cited above (Danard 1964) for syncptic charts and other details of the case studied.

Fig. 6 shows the net flux (positive upward) at 300 mb. The top of the principal cloud deck is clearly delineated by relatively low values of flux. Its lateral boundary is given approximately by the isopleth $F = 1.75 \times 10^5$ ergs sec^{-1} cm^{-2}.

Figs. 7-9 show the rate of loss of energy due to long-wave radiation from water vapor. By far the greatest loss occurs in the upper portion of the cloud mass. The large values in the Oklahoma-Kansas region at 800 mb (Fig. 9) indicate strong cooling at the top of stratocumulus cloud with clear skies above. Zero values mean that the

point in question is in cloud. Negative values indicate warming beneath cloud or in the lower portion of the cloud mass. For comparison with the results of Section 4, 1 C day^{-1} = 1.17 x 10^2 ergs $gm^{-1}sec^{-1}$.

Figs. 7-9 are to be compared with Fig. 8 of Danard (1964). The latter depicts the rate of release of latent heat at 400, 600 and 800 mb. This was largest in the Indiana-Pennsylvania area and amounted to about 3 x 10^3 ergs $gm^{-1}sec^{-1}$ at 400 and 800 mb and about 5 x 10^3 ergs $gm^{-1}sec^{-1}$ at 600 mb. Thus in the case studied, the long-wave cooling at cloud top was smaller by a factor of about five than the maximum rate of release of latent heat in the upper troposphere. It may be remarked that this case was one of heavy precipitation and in less intense cyclones, the ratio would be smaller. However, in the middle and lower troposphere, radiative loss was generally negligible in the region of precipitation compared to release of latent heat.

The long-wave cooling at cloud top amounts to 5.4 C day^{-1} in the upper 200 mb of the cloud mass (Fig. 7). This latter figure agrees qualitatively with the estimate of Moller (1951). The cooling would tend to be offset by absorption of solar radiation at cloud top. However, many workers (e.g., Moller (1951) or London (1957)) regard this effect as small. The long-wave cooling at cloud top greatly exceeds that in the cloud-free air. Thus an accurate computation of the latter may be relatively unessential in the study of cyclogenesis over short time intervals (say 48 hrs or less).

The temperature difference between 800 and 400 mb at the location of the sea-level low (southern Illinois) is 31 C. By comparison, if the lapse-rate were pseudo-adiabatic, the value would be 34 C. Neglecting effects of vertical motion and differential advection, and assuming that the pattern of computed radiative cooling moves with

the cyclone, the 800-400 mb temperature difference at the surface low would be 36 C after 24 hrs. This represents a conditionally unstable state which would presumably be alleviated by convective overturning.

6. Concluding remarks

A possible modification to the treatment of clouds would be to allow for fractional amounts in each layer. However, this would complicate the calculations unless the number of layers in the vertical were kept small.

Short-wave absorption by water vapor is appreciable in the lower troposphere at low latitudes (see Section 4). The average heating due to this source could be included if desired.

The question of the influence of long-wave radiation on the evolution of cyclones is probably best answered by comparative numerical integrations. Cooling and destabilization of the upper part of the cloud mass are to be expected. Destabilization and subsequent increase in precipitation may be important in the dynamics of development.

Acknowledgments

The author wishes to express his thanks to Professor Frank L. Martin for helpful discussion throughout this study. The research was supported by the U.S. Air Force Cambridge Research Laboratories under Research Project MIPR ES-7-967.

REFERENCES

Brooks, D.L., 1950: A tabular method for the computation of temperature change by infrared radiation in the free atmosphere. J. Meteor., 7, 313-321.

Danard, M.B., 1964: On the influence of released latent heat on cyclone development. J. Appl. Meteor., 3, 27-37.

_____, 1966a: A quasi-geostrophic numerical model incorporating effects of release of latent heat. J. Appl. Meteor., 5, 85-93.

_____, 1966b: Further studies with a quasi-geostrophic numerical model incorporating effects of released latent heat. J. Appl. Meteor., 5, 388-395.

Davis, P.A., 1963: An analysis of the atmospheric heat budget. J. Atmos. Sci., 1, 5-22.

Goody, R.M., 1964: Atmospheric radiation - I - theoretical basis. London, Oxford Univ. Press, 436 pp.

Haltiner, G.J., and F.L. Martin, 1957: Dynamical and physical meteorology. New York, McGraw-Hill, 470 pp.

Kuhn, P.M., 1963a: Measured effective long-wave emissivity from clouds. Mon. Wea. Rev., 91, 635-640.

_____, 1963b: Soundings of observed and computed flux. J. Geophys. Res., 68, 1415-1420.

_____, 1963c: Radiometersonde observations of infrared flux emissivity of water vapor. J. Appl. Meteor., 2, 368-378.

London, J., 1957: A study of the atmospheric heat balance. Final Rep., Contract No. AF 19(122)-165, Dept. of Meteor. and Ocean., New York Univ., July 1957, 99 pp. (ASTIA No. 117227)

Manabe, S., and F. Moller, 1961: On the radiative equilibrium and heat balance of the atmosphere. Mon. Wea. Rev., 89, 503-532.

Manabe, S., and R.F. Strickler, 1964: Thermal equilibrium of the atmosphere with a convective adjustment. J. Atmos. Sci., 21, 361-385.

Moller, F., 1951: Long-wave radiation. Compendium of Meteorology (T.F. Malone ed.), Boston, Amer. Meteor. Soc., 34-49.

Smagorinsky, J., 1960: On the dynamical prediction of large-scale condensation by numerical methods. Physics of Precipitation (H. Weickmann ed.), Geophy. Mon. No. 5, Washington, Amer. Geophy. Union, 71-78.

Legends for Figures

Fig. 1. Schematic diagram showing levels referred to in Eq. (3).

Fig. 2. Schematic diagram showing levels at which terms in Eqs. (3) and (9) are computed in Section 3.

Fig. 3. Configurations of cloud in the model atmosphere of Section 3. Hatching denotes cloud.

Fig. 4. Annual average cooling rates for a cloudless atmosphere associated with long-wave radiation from water vapor. Units: deg C day^{-1}.

Fig. 5. Difference between cooling rates of Fig. 4 and those of Manabe and Moller (1961), who include both long- and short-wave radiation. Units: deg C day^{-1}.

Fig. 6. Net upward flux at 300 mb. 1200 GMT 21 January 1959. Units: 10^5 ergs sec^{-1} cm^{-2}.

Fig. 7. Net loss of radiative energy per unit mass at 400 mb. 1200 GMT 21 January 1959. Units: 10^2 ergs gm^{-1} sec^{-1}.

Fig. 8. As in Fig. 7 but for 600 mb.

Fig. 9. As in Fig. 7 but for 800 mb.

Fig. 1

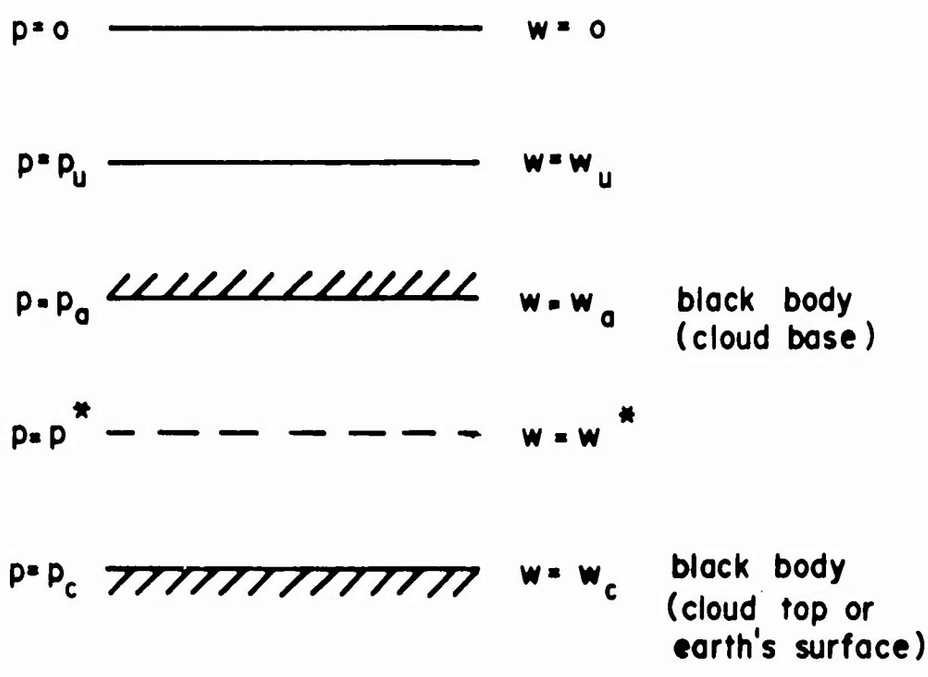
p = o
w = o
p = p_u
w = w_u
p = p_a
w = w_a
black body
(cloud base)
p = p^*
w = w^*
p = p_c
w = w_c
black body
(cloud top or
earth's surface)

Fig. 2

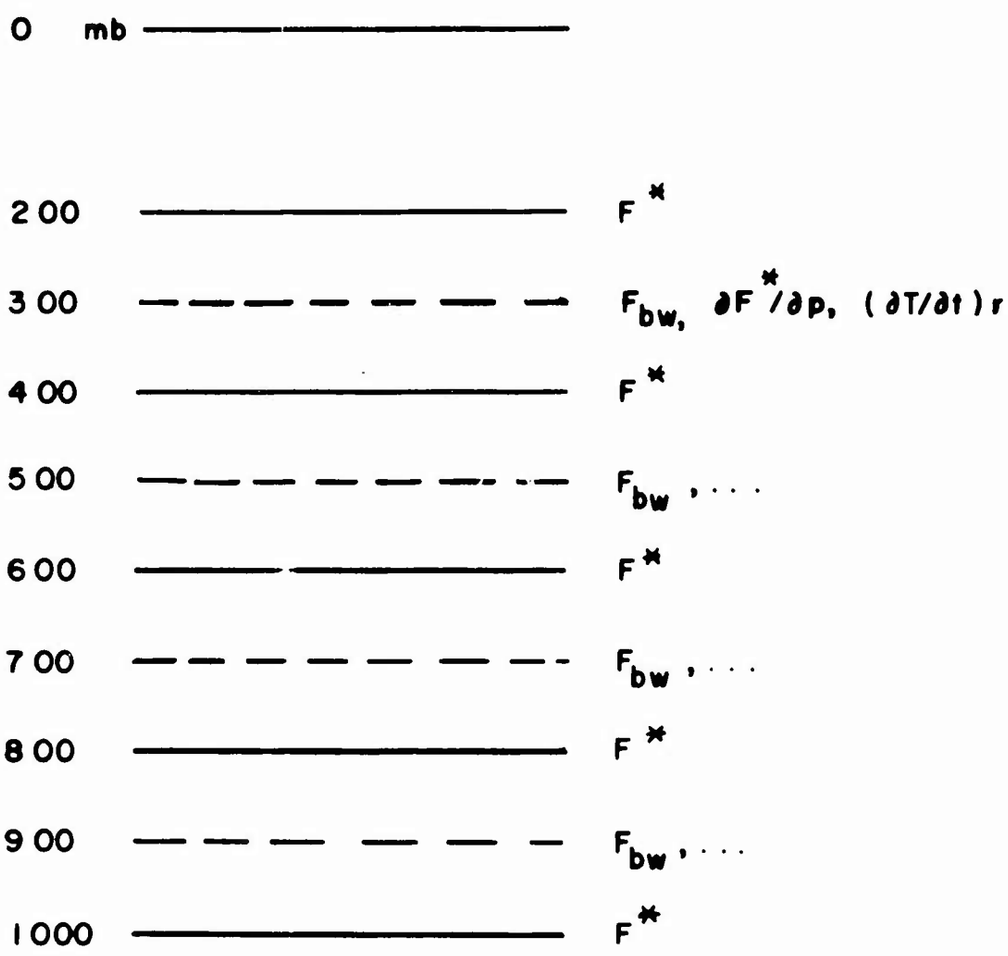
0 mb
200
300
400
500
600
700
800
900
1000
F^*
F_{bw}, $\partial F^*/\partial p$, $(\partial T/\partial t)_r$
F^*
F_{bw}, ...
F^*
F_{bw}, ...
F^*
F_{bw}, ...
F^*

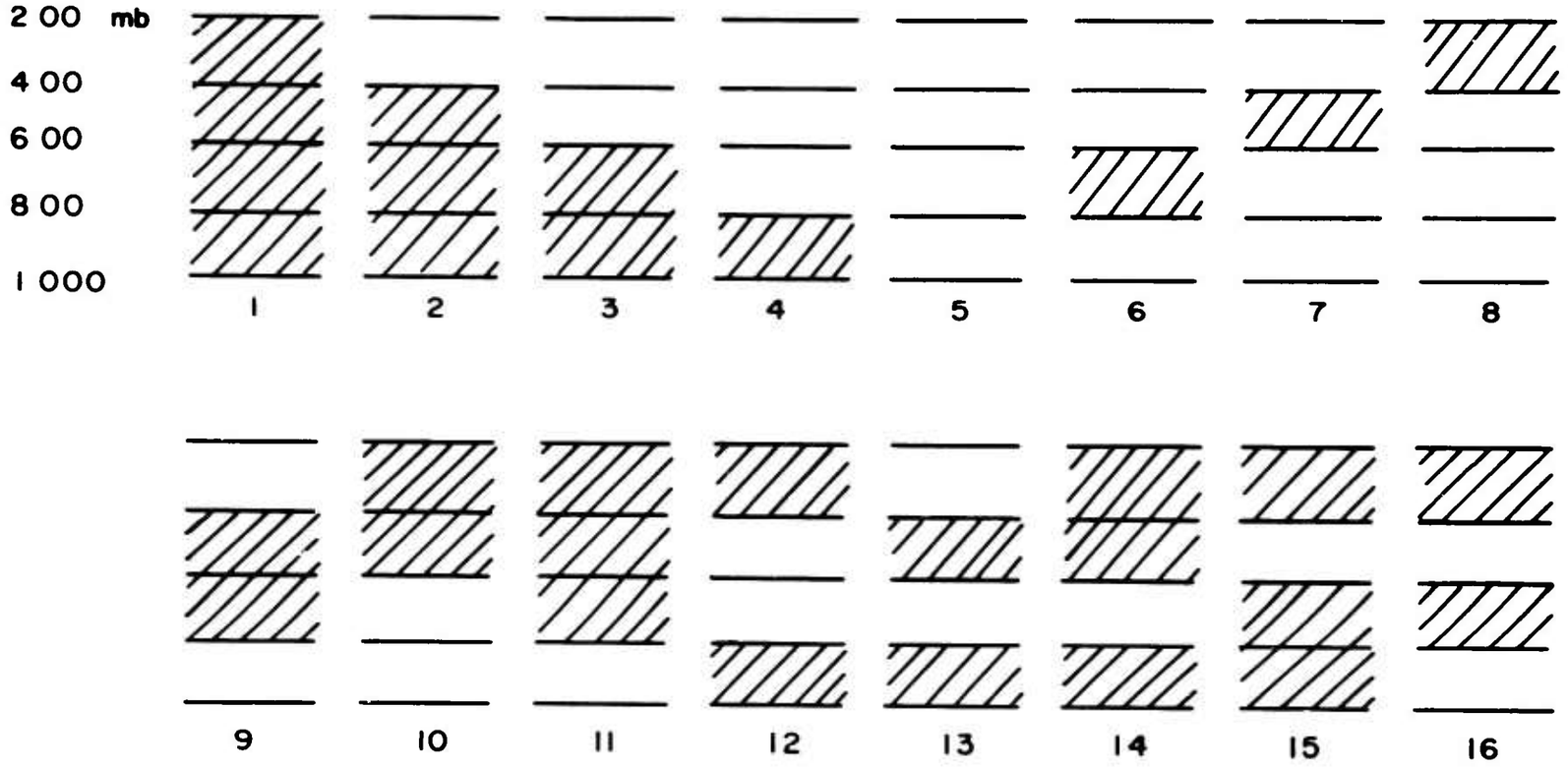

Fig. 3

Fig. 4

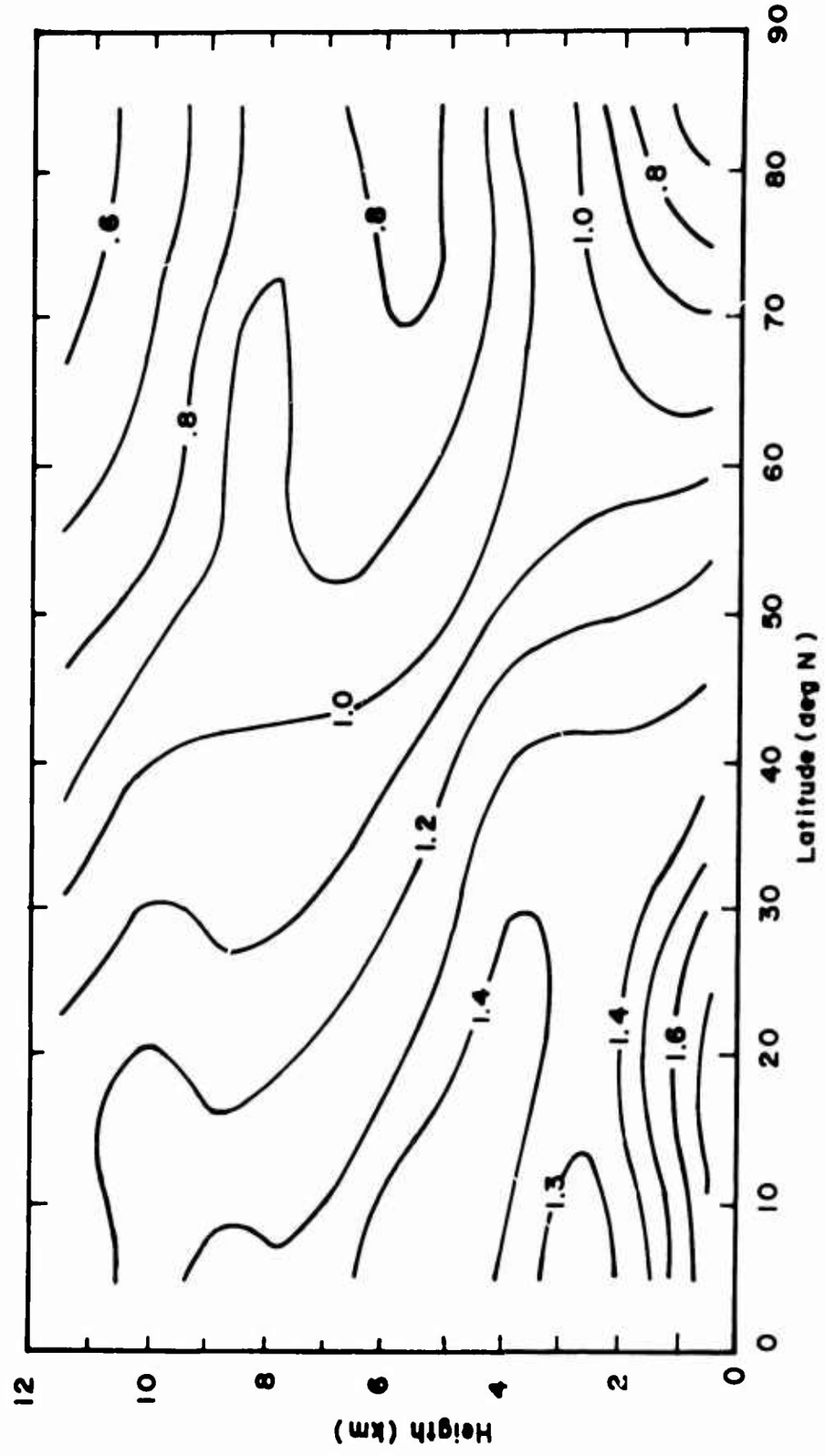

Fig. 5

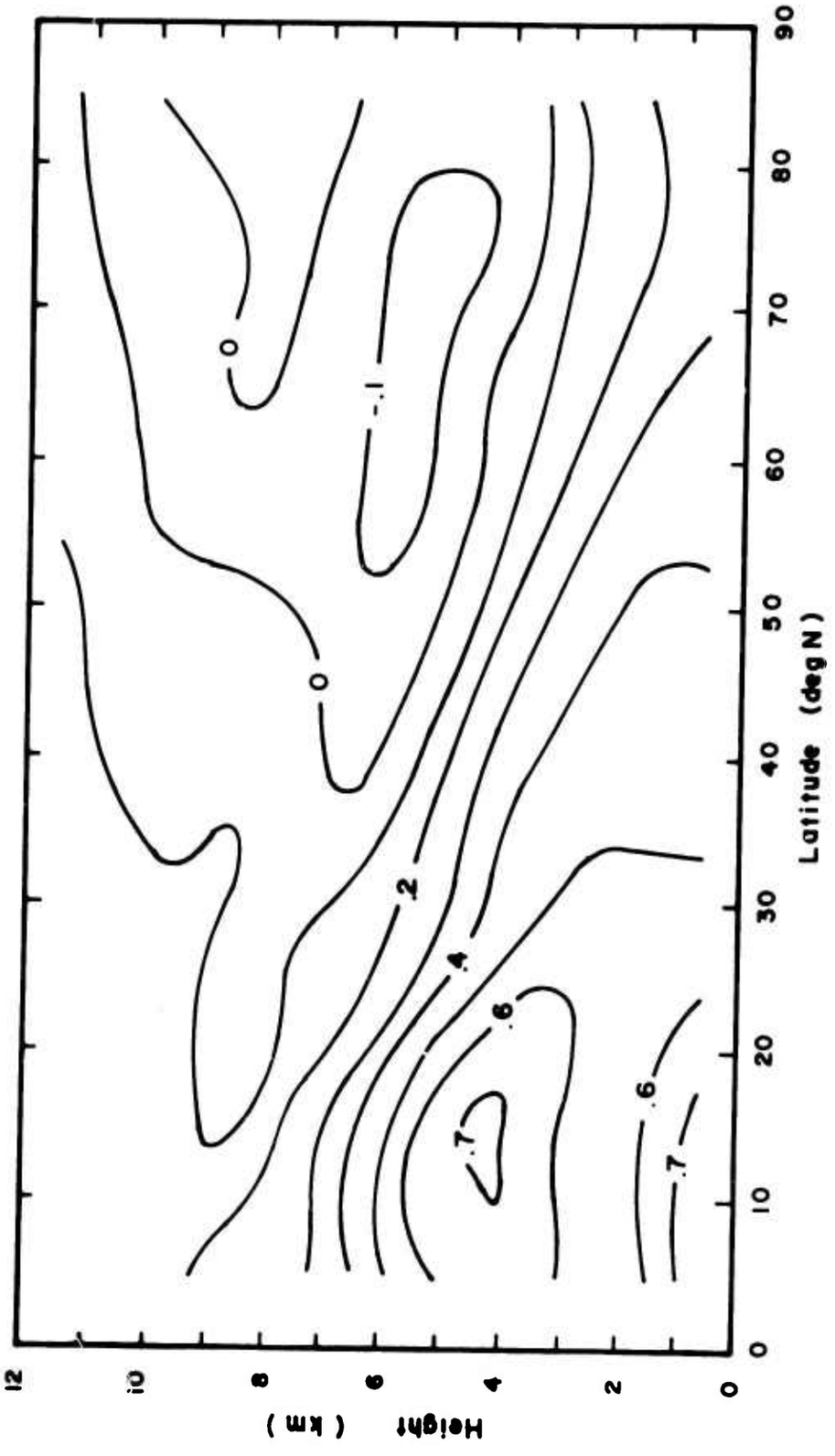
Height (km)
0
2
4
6
8
10
12
Latitude (deg N)
0
10
20
30
40
50
60
70
80
90
0
-.1
.2
.4
.6
.7
.6
.7

Fig. 6

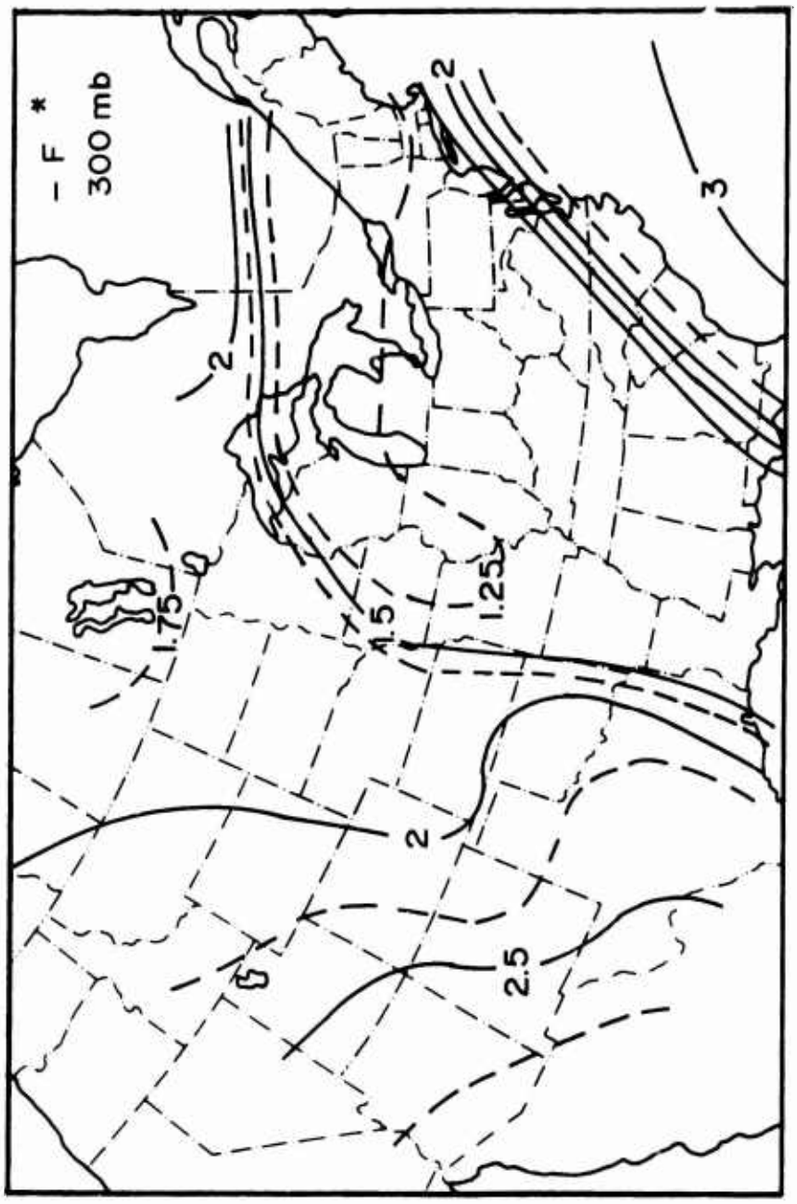

Fig. 7

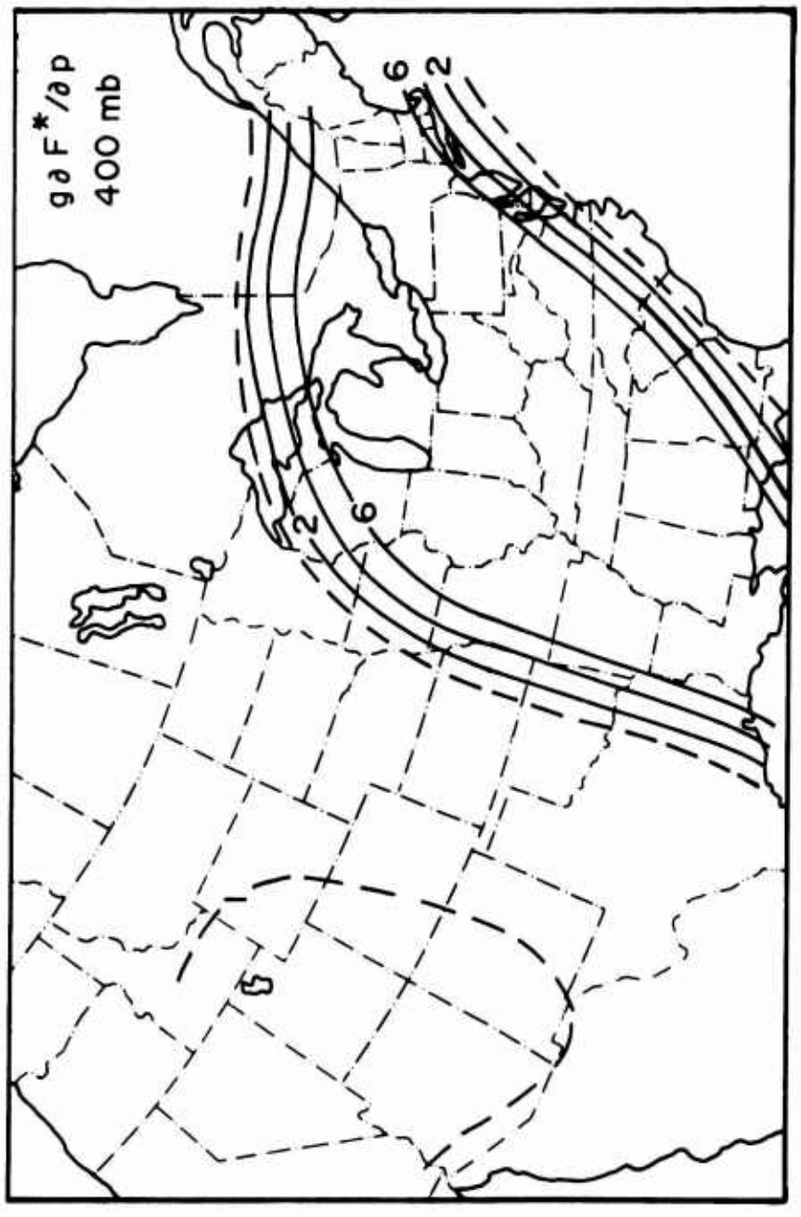

Fig. 8

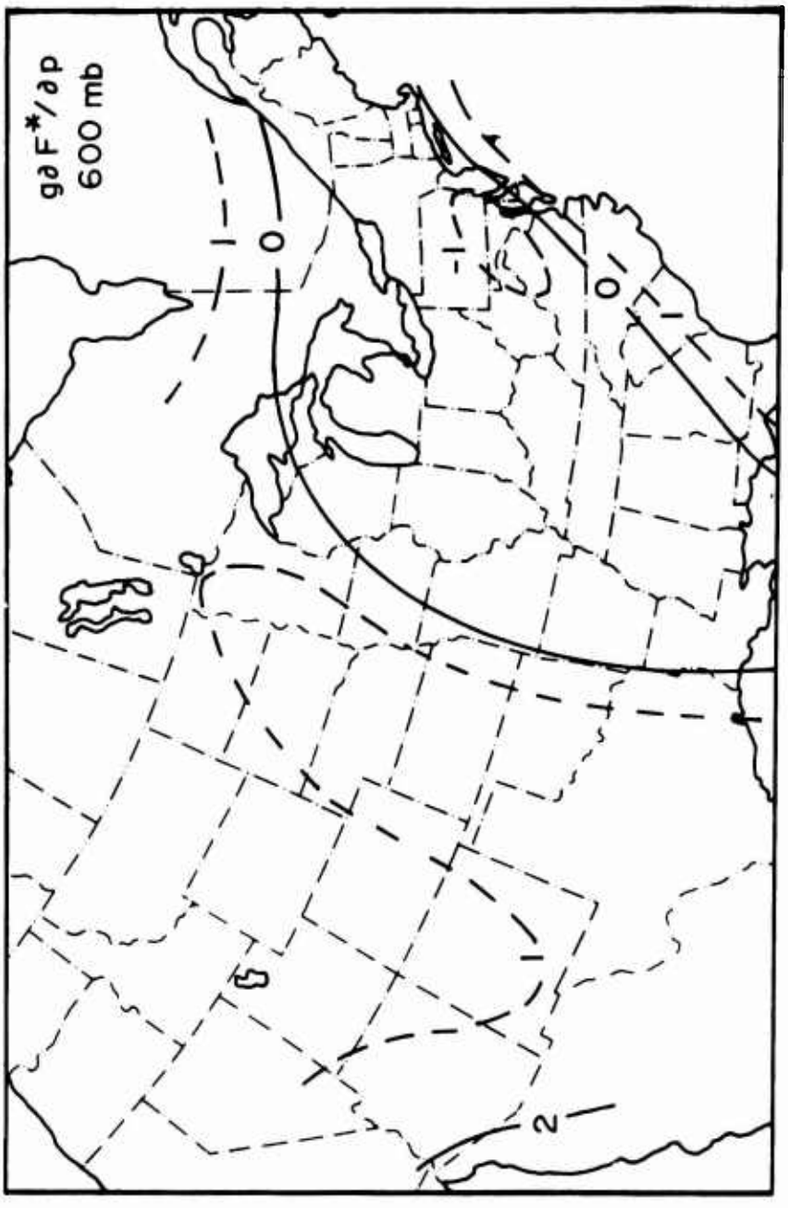

Fig. 9

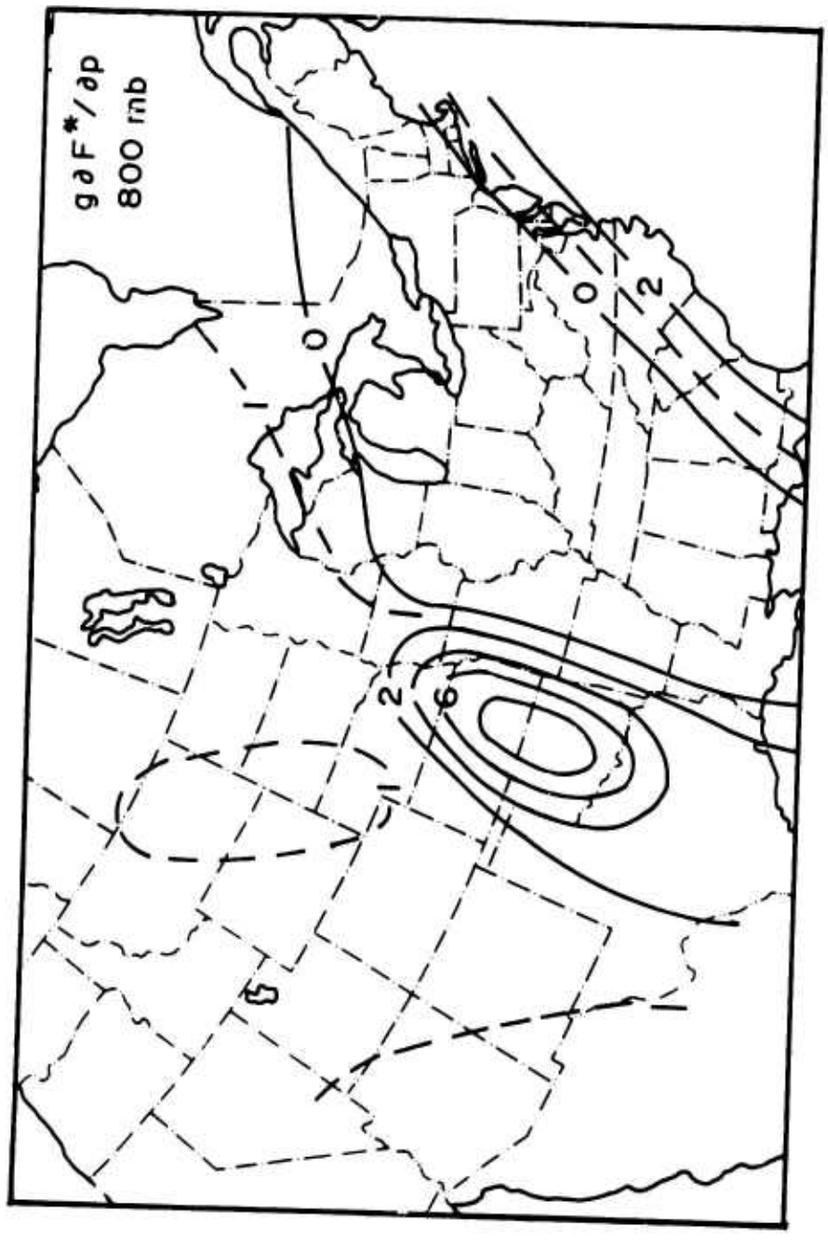

Unclassified

Security Classification

DOCUMENT CONTROL DATA - R & D

Security classification of title, body of abstract and indexing annotation must be entered when the overall report is classified)

1. ORIGINATING ACTIVITY (Corporate author)
Naval Postgraduate School
Dept. of Meteorology and Oceanography
Monterey, California 93940

2a. REPORT SECURITY CLASSIFICATION
Unclassified

2b. GROUP

3. REPORT TITLE
ON THE INCLUSION OF LONG-WAVE RADIATION IN A TROPOSPHERIC NUMERICAL PREDICTION MODEL

4. DESCRIPTIVE NOTES (Type of report and, inclusive dates)
Scientific. Interim.

5. AUTHOR(S) (First name, middle initial, last name)
Maurice B. Danard

6. REPORT DATE	7a. TOTAL NO OF PAGES	7b. NO OF REFS
January 1968	32	15

8a. CONTRACT OR GRANT NO	9a. ORIGINATOR'S REPORT NUMBER(S)
MIPR ES-7-967 b. PROJECT XX, Task, Work Unit Nos. 6698-02-01 c. DoD Element 62405394 d. DoD Subelement 681000	NPS-51DD8011A Scientific Report No. 1 9b. OTHER REPORT NO(S) (Any other numbers that may be assigned this report) AFCRL-68-0018

10. DISTRIBUTION STATEMENT
Distribution of this document is unlimited. It may be released to the Clearinghouse, Department of Commerce, for sale to the general public.

11. SUPPLEMENTARY NOTES	12. SPONSORING MILITARY ACTIVITY
TECH, OTHER	Air Force Cambridge Research Laboratories (CRH), L.G. Hanscom Field, Bedford, Massachusetts 01730

13. ABSTRACT

A simple method of computing long-wave radiative cooling in the troposphere associated with water vapor is described. Radiation from ozone and carbon dioxide is not considered. However, influences of arbitrary vertical distributions of cloud and moisture are included.

Average annual cooling rates along a meridional cross-section are calculated for a cloudless atmosphere. The results agree fairly well with the total radiative cooling (long- and short-wave) as given by Manabe and Moller (1961) except in the lower troposphere at low latitudes. Here short-wave absorption by water vapor is appreciable.

Long-wave radiative cooling is also computed in a case of a developing cyclone for comparison with release of latent heat. The largest cooling occurs at cloud top and can be a significant fraction of the amount of energy released as latent heat in the upper troposphere. Destabilization of the cloud mass and subsequent increase in precipitation may be important in cyclone development.

DD FORM 1 NOV 65 1473 (PAGE 1)

S/N 0101-807-6811

Unclassified

Security Classification

A-31408

14 KEY WORDS	LINK A		LINK B		LINK C	
	ROLE	WT	ROLE	WT	ROLE	WT
Tropospheric long-wave radiation						
Numerical modelling						
Water vapor emissivities						
Cloud destabilization						